Supporting Information

Nitrogen-mediated growth of silver nanocrystals to form ultra-thin, high-purity silver film electrodes with broadband transparency for solar cells

Guoqing Zhao,[†] Wenfei Shen,[‖] Eunwook Jeong,[†] Sang-Geul Lee,[‡] Hee-Suk Chung,[±] Tae-Sung Bae,[±] Jong-Seong Bae,[§] Gun-Hwan Lee,[†] Jianguo Tang,*[,‖] and Jungheum Yun*[,†]

[†]Surface Technology Division, Korea Institute of Materials Science, Changwon, Gyeongnam 51508, Republic of Korea

[‖]Academy of Hybrid Materials, National Base of International Science & Technology Cooperation on Hybrid Materials, Qingdao University, Qingdao 266071, People's Republic of China

[‡]Daegu Center, Korea Basic Science Institute, Daegu, 41566, Republic of Korea

[±]Jeonju Center, Korea Basic Science Institute, Jeonju, Jeonbuk 54907, Republic of Korea

[§]Busan Center, Korea Basic Science Institute, Busan, 46742, Republic of Korea

*Corresponding authors: jungheum@kims.re.kr; jianguotangde@hotmail.com.

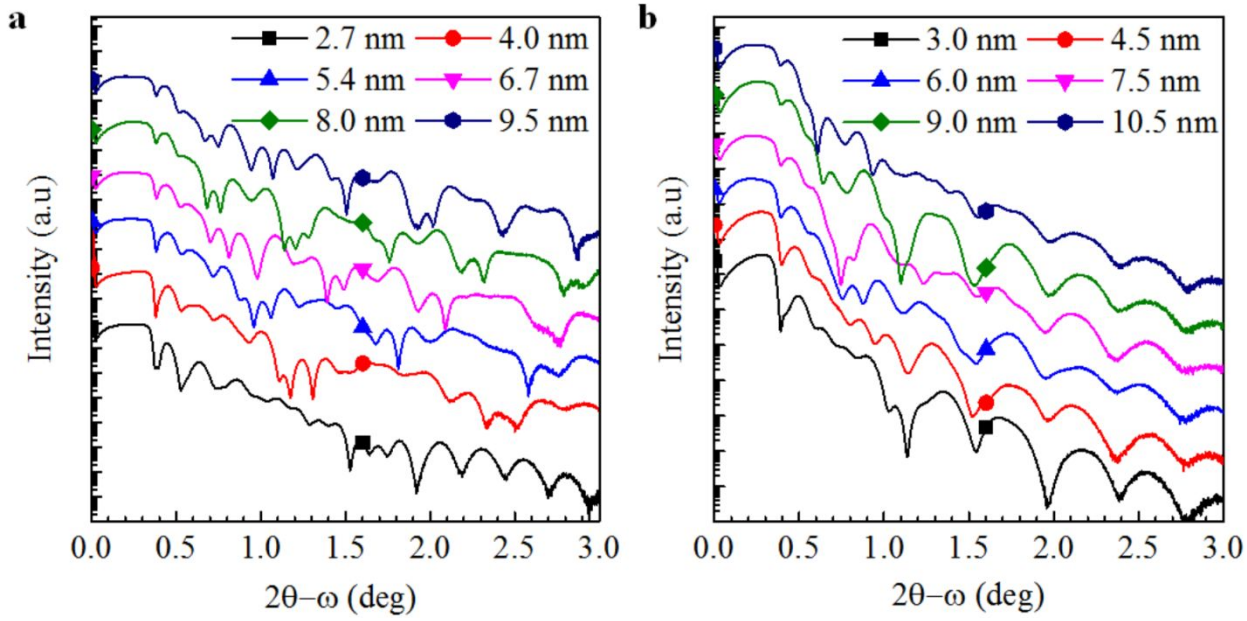

Figure S1. X-ray reflectivity spectra measured for (a) Ag_N and (b) Ag of different thicknesses in ZnO/Ag_N/ZnO and ZnO/Ag/ZnO configurations.

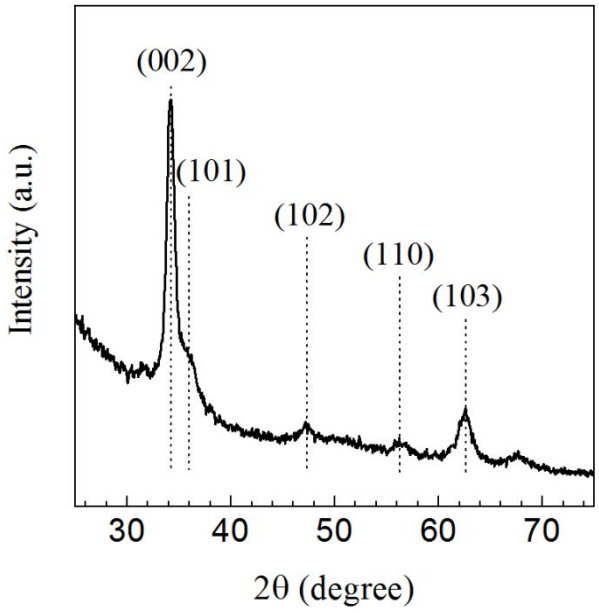

Figure S2. X-ray diffraction pattern of 2θ scan measured for a 15-nm ZnO film deposited on a PET substrate with the conditions corresponding to those described in Figure 3.

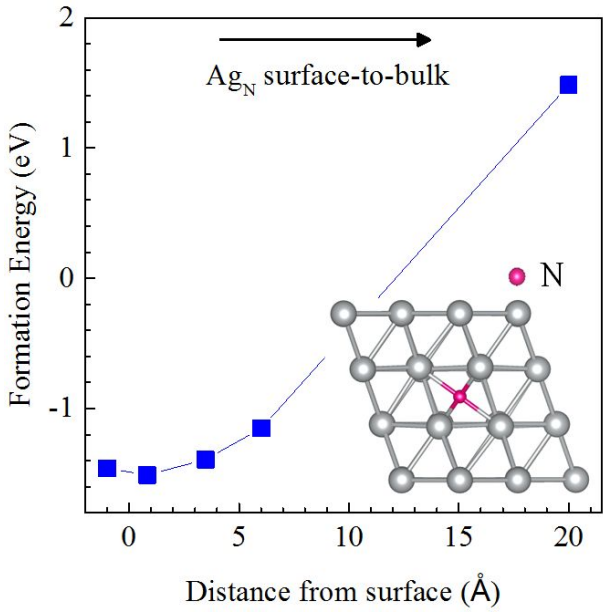

Figure S3. Numerically predicted formation energy of a nitrogen atom occupying an interstitial-octahedral site in a Ag(111) domain with a geometric configuration shown in the inset as a function of the distance (depth) perpendicular to the surface into the bulk of the Ag(111) domain. The formation energies were determined by calculating the total energy, as follows: $\Delta E_{\mathrm{f}} = E_{\mathrm{Ag_N}} - (E_{\mathrm{Ag}} + \Delta n_{\mathrm{Ag}} \mu_{\mathrm{Ag}} + \Delta n_{\mathrm{N}} \mu_{\mathrm{N}})$, where $E_{\mathrm{Ag_N}}$ and E_{Ag} denote the total energy of the Ag slab system incorporating and not incorporating a single nitrogen atom, respectively, Δn_{Ag} and Δn_{N} respectively denote the number of positive or negative Ag and nitrogen atoms in the $\mathrm{Ag_N}$ slab system, and μ_{Ag} and μ_{N} are the chemical potentials of Ag and nitrogen, respectively. The chemical potential of the nitrogen was approximated from the total energy of an N_2 molecule as follows: $\mu_{\mathrm{N}} = \frac{1}{2}\mu_{\mathrm{N_1}} + 4\mathrm{eV}$, where $\mu_{\mathrm{N_2}}$ is the total energy of a nitrogen molecule. The chemical potential of the Ag was determined from the total energy of the bulk Ag.

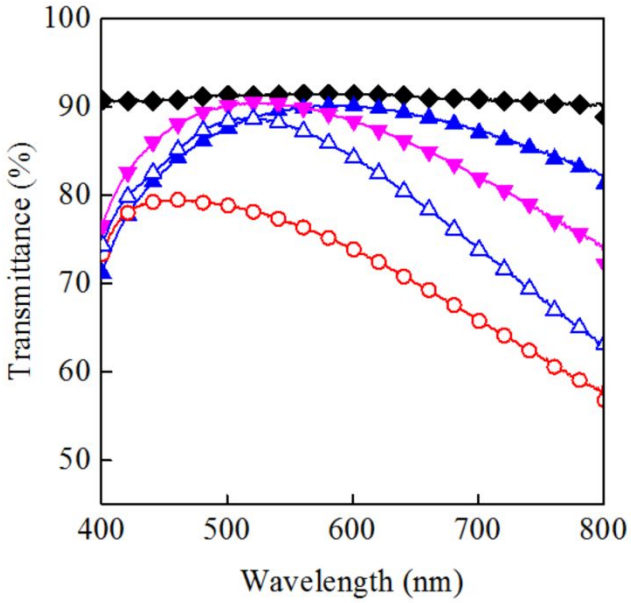

Figure S4. Total transmittance, measured by including reference spectrum of glass substrate (black diamonds), of ZANZ and ZAZ TEs with various Ag_N and Ag thicknesses: 5.4-nm Ag_N (solid, blue upward-pointing triangles), 6.7-nm Ag_N (solid, magenta downward-pointing triangles), 6.0-nm Ag (open, red circles), 9.0-nm Ag (open, blue upward-pointing triangles), which correspond to the conditions described in Figure 5b. The thicknesses of the top cover and bottom supporting ZnO films were fixed to 5 and 25 nm, respectively.

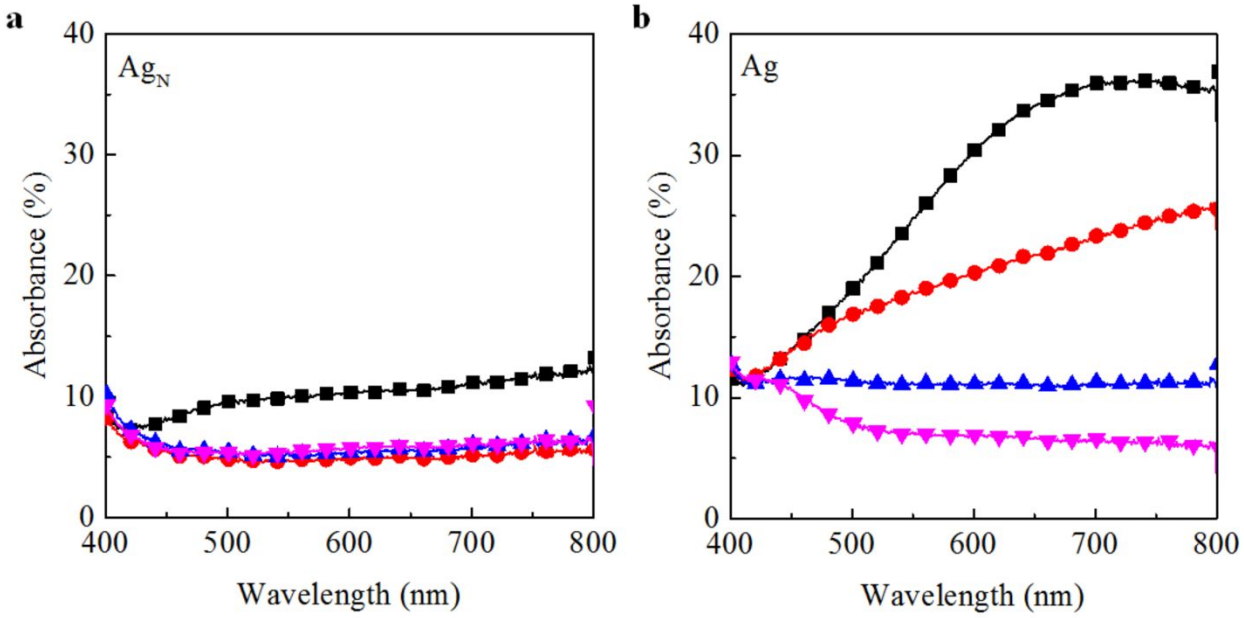

Figure S5. Absorbance, 100 − Transmittance (%) − Reflectance (%), of (a) ZANZ and (b) ZAZ TEs deposited on glass with various Ag_N and Ag thicknesses: 2.7-nm Ag_N and 3.0-nm Ag (black squares), 4.0-nm Ag_N and 6.0-nm Ag (red circles), 5.4-nm Ag_N and 7.5-nm Ag (blue upward-pointing triangles), and 6.7-nm Ag_N and 9.0-nm Ag (magenta downward-pointing triangles), which correspond to the conditions described in Figure 5b.

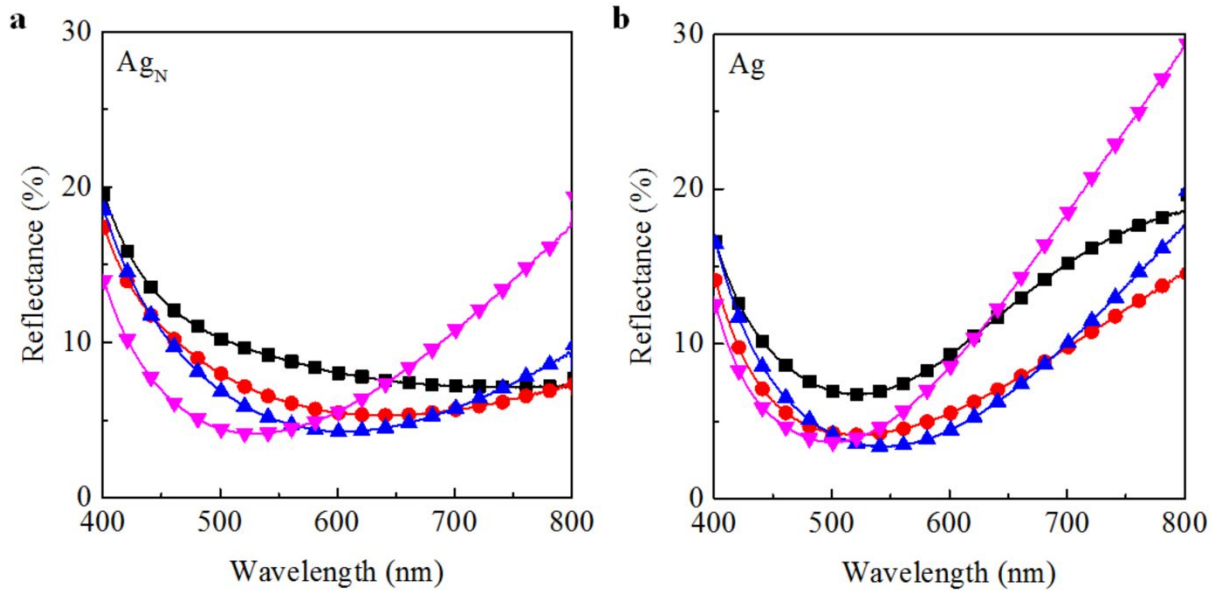

Figure S6. Total reflectance of (a) ZANZ and (b) ZAZ TEs deposited on glass with various Ag_N and Ag thicknesses: 2.7-nm Ag_N and 3.0-nm Ag (black squares), 4.0-nm Ag_N and 6.0-nm Ag (red circles), 5.4-nm Ag_N and 7.5-nm Ag (blue upward-pointing triangles), and 6.7-nm Ag_N and 9.0-nm Ag (magenta downward-pointing triangles), which correspond to the conditions described in Figure 5b.

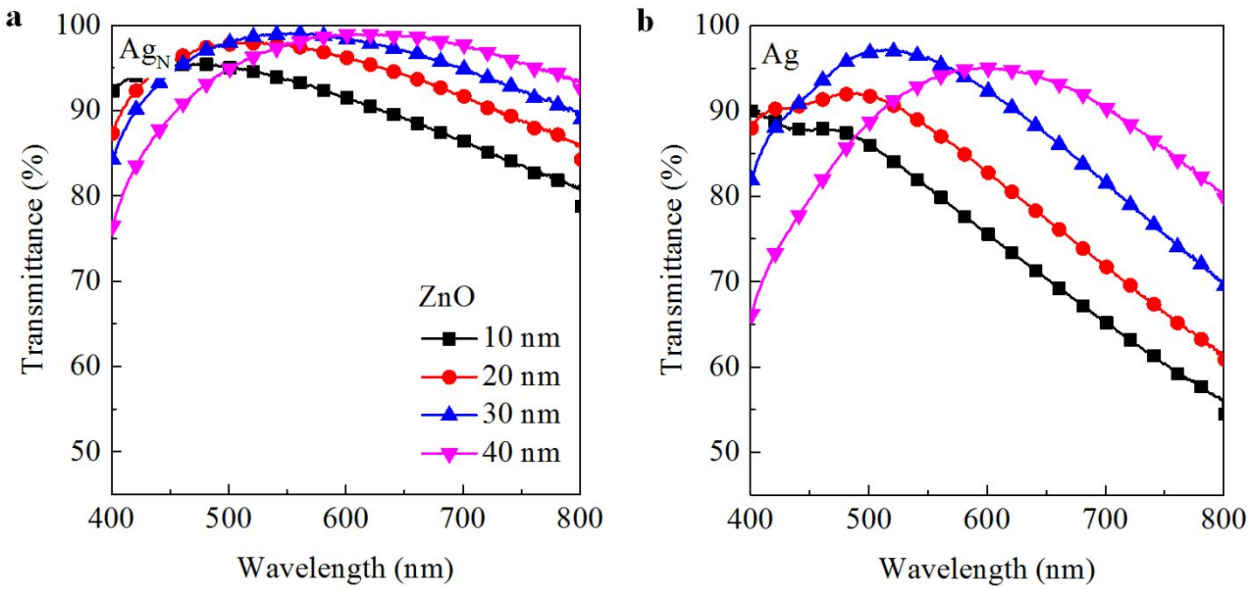

Figure S7. Changes in the total transmittance of (a) ZANZ and (b) ZAZ TEs deposited on glass with 5.4-nm Ag_N and 9.0-nm Ag, respectively, as function of the thickness of the covering ZnO film. The thickness of the ZnO supporting film was fixed to 5 nm.

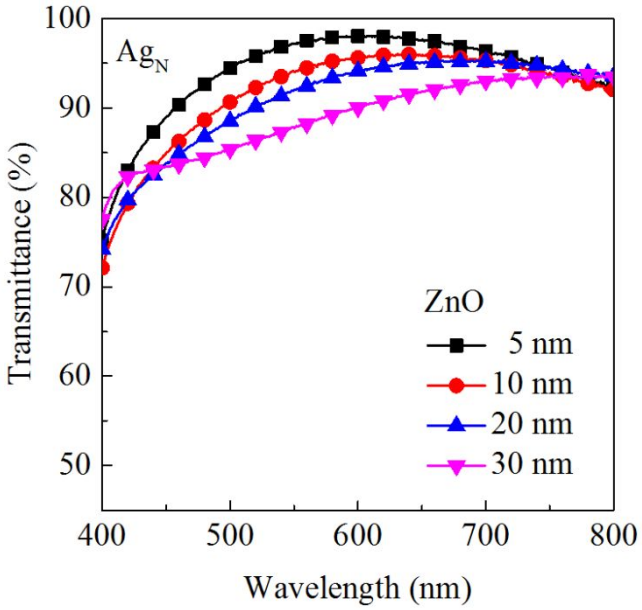

Figure S8. Change in the total transmittance of ZANZ TE deposited on glass with 5.4-nm Ag_N and 25-nm top ZnO layers as a function of the thickness of the bottom ZnO film.

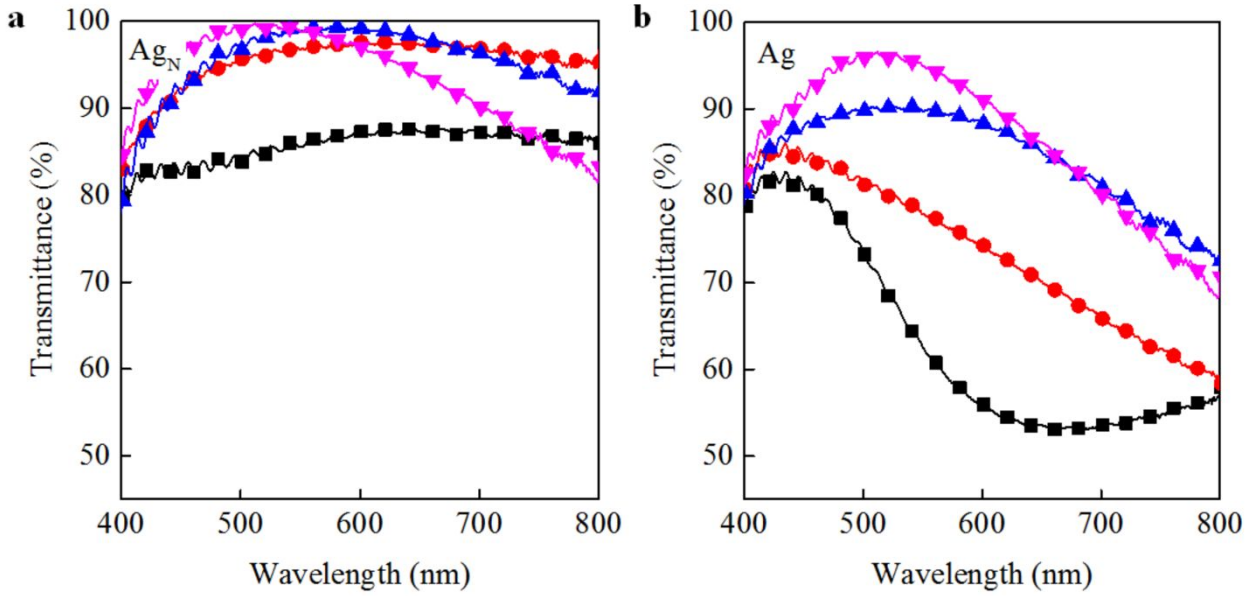

Figure S9. Total transmittance of (a) ZANZ and (b) ZAZ TEs deposited on PET polymer substrates with various Ag_N and Ag thicknesses: 2.7-nm Ag_N and 3.0-nm Ag (black squares), 4.0-nm Ag_N and 6.0-nm Ag (red circles), 5.4-nm Ag_N and 7.5-nm Ag (blue upward-pointing triangles), and 6.7-nm Ag_N and 9.0-nm Ag (magenta downward-pointing triangles), which correspond to the conditions described in Figure 5b.

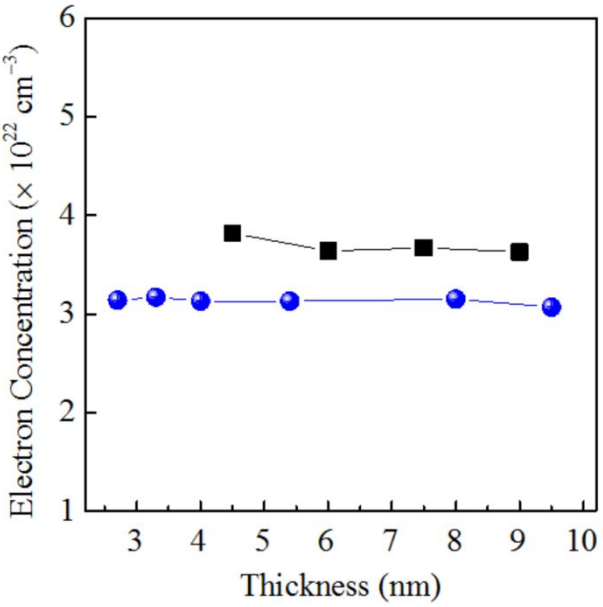

Figure S10. Electron concentration of ZANZ and ZAZ TEs as a function of the thickness of Ag_N (blue circles) and Ag (black squares), which correspond to the conditions described in Figure 5d. The solid lines are provided for clarity.

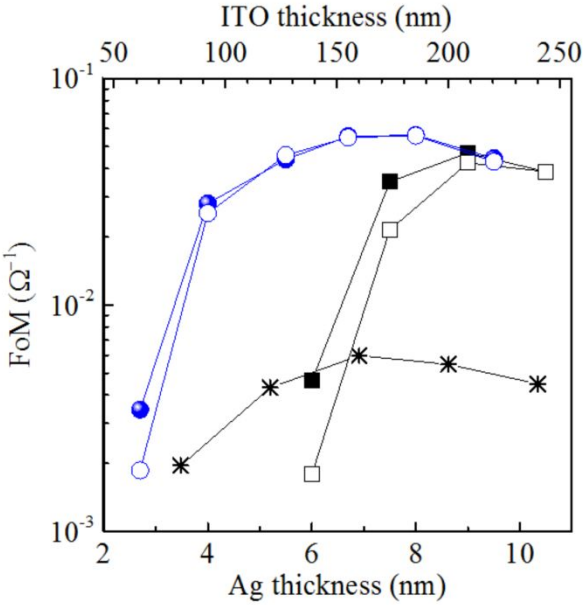

Figure S11. Figure of merit (FoM), T^{10}/R_S, where T is the average total transmittance for the overall visible spectral ranges between 400–800 nm, and R_S is the sheet resistance of ZANZ (blue circles), ZAZ (black squares) and amorphous ITO (black stars) TEs. The FoM were determined for ZANZ and ZAZ TEs supported on glass (solid) and PET (open) substrates, and compared with amorphous ITO single-film TEs supported on PET substrates. The solid lines are added for clarity.

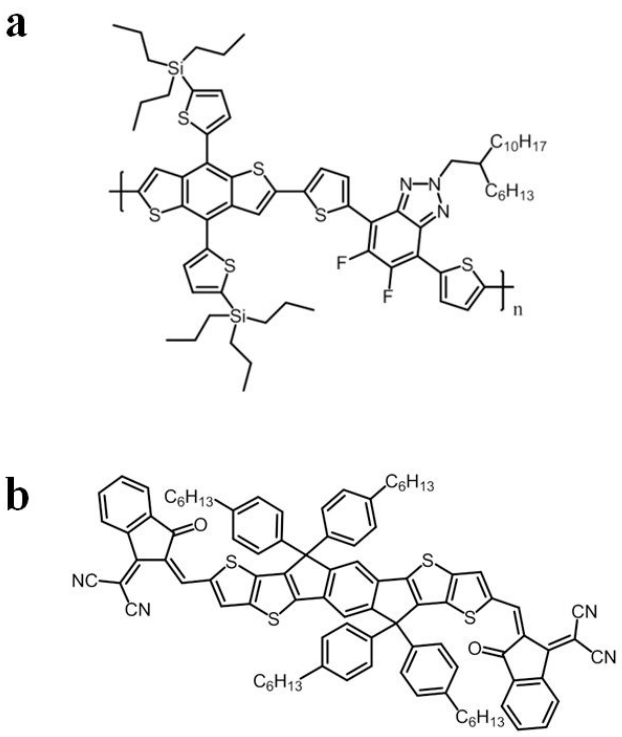

Figure S12. Chemical structural information for (a) J71 and (b) ITIC applied to the photoactive blend layer as the donor and the acceptor, respectively.

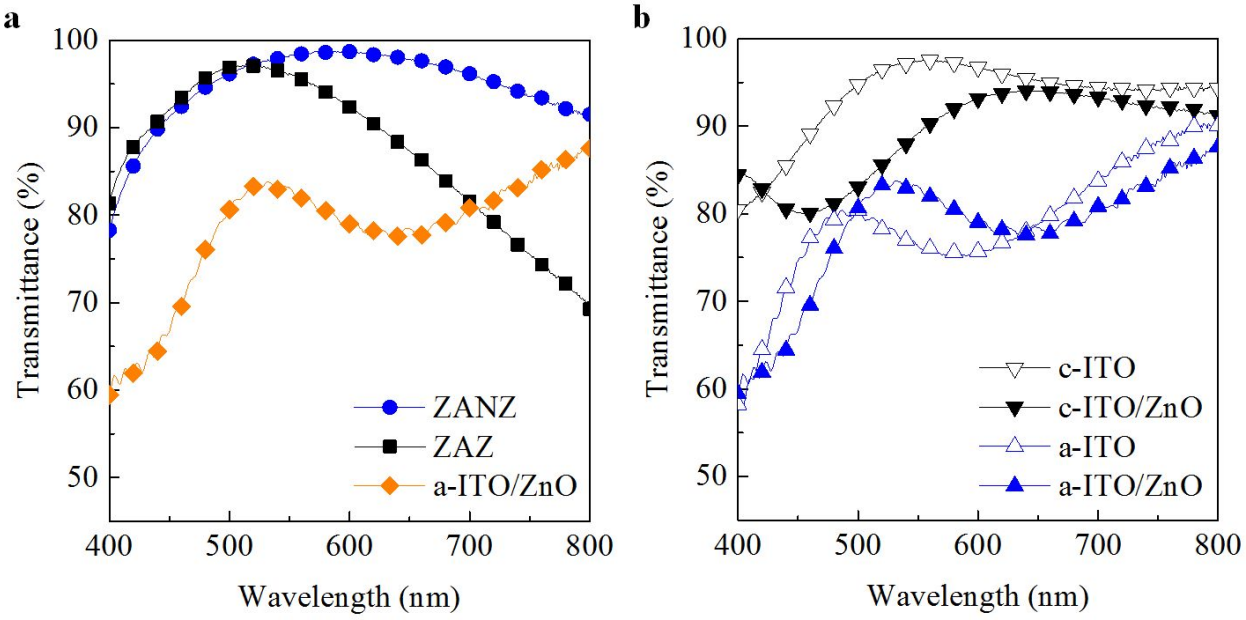

Figure S13. Comparison of the total transmittance spectra of (a) three different TEs applied for flexible OSCs: a ZANZ TE with a 5.4-nm AgN layer, a ZAZ TE with a 9.0-nm Ag layer, and a 240-nm amorphous ITO layer coated with a 25-nm top covering ZnO electron transport layer (a-ITO/ZnO) and (b) a 150-nm crystalline ITO layer supported on a glass substrates and a 240-nm amorphous ITO layer supported on a PET substrate with and without the top ZnO layer.

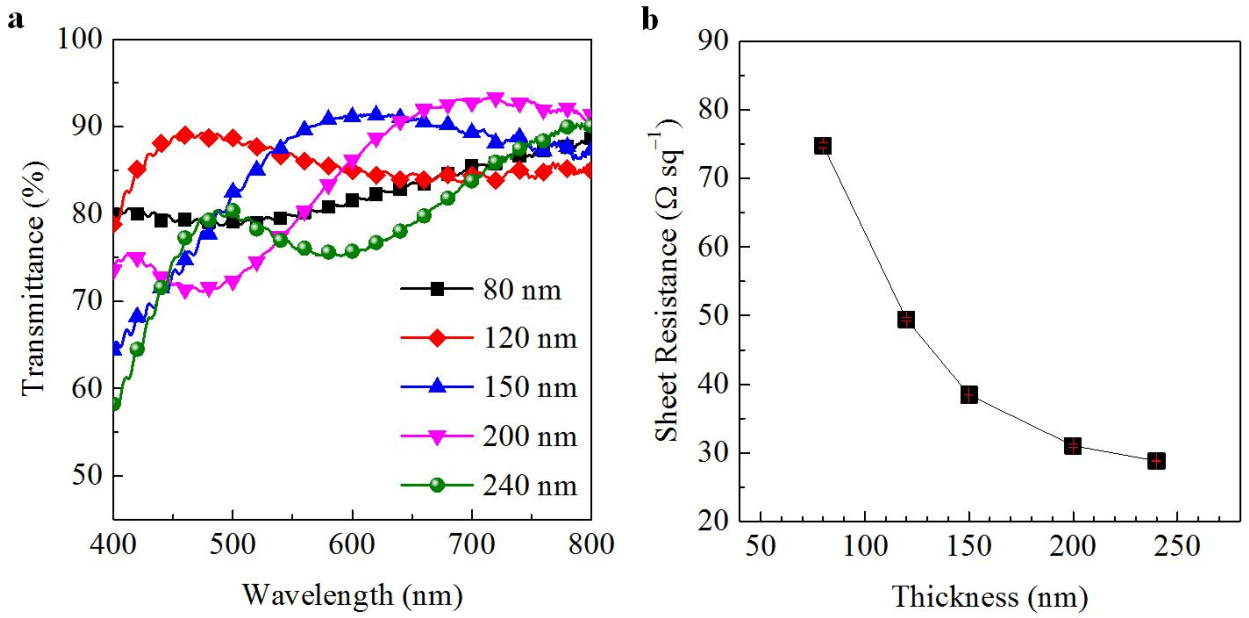

Figure S14. Changes in (a) total transmittance spectra and (b) sheet resistance of amorphous ITO single-film TEs of different thicknesses, supported on PET substrates.